JOURNAL OF APPLIED ELECTROCHEMISTRY 23 (1993) 379–386

Effect of cobalt deposits on nickel substrates on the oxygen evolution reaction in KOH

L. BROSSARD, C. MESSIER

Institut de Recherche d'Hydro-Québec (IREQ), 1800 montée Ste-Julie, Varennes, Québec, Canada J3X 1SI

Received 24 February 1992; revised 14 August 1992

Cobalt deposits taking the form of cobalt nodules were obtained on nickel substrates in a bath containing dissolved cobalt sulphate and ammonium citrate at pH 9.8 and 23° C. Oxygen discharge was investigated on those electrodes in 40 wt % KOH solution at temperatures ranging between 40 and 80° C. Up to a cobalt loading of 12 mg cm^{-2}, the larger the loading, the larger the electrode/solution interface, which resulted in improved electrocatalytic activity with the loading. The electrocatalytic activity was also largely temperature-dependent.

1. Introduction

The high overpotential of the oxygen evolution reaction (o.e.r.) is one of the dominant factors contributing to lower performance in alkaline water electrolysis [1, 2]. Cobalt coatings were recently obtained on nickel substrate by electrodeposition of cobalt in 30 wt % KOH at 25° C [3]. Cobalt was introduced in the form of tris-ethylenediamine cobalt (III) chloride prior to deposition. The oxygen overpotential at 0.25 A cm^{-2} in 30 wt % KOH at 70° C is ~0.32 V when the cobalt loading is 4.6 mg cm^{-2}. The morphology of the cobalt coatings is favorable for the o.e.r. and the intrinsic electrocatalytic activity is higher for cobalt than for nickel [4].

One of the major problems with the use of tris-ethylenediamine cobalt (III) chloride to obtain cobalt deposits in concentrated alkaline solutions is its decomposition time, in terms of days, which makes it difficult to reproduce the coating characteristics. An alternative is to use solutions with a lower pH or which contain dissolved inorganic compounds of cobalt [5].

The present investigation deals with the o.e.r. on cobalt coatings electrodeposited on nickel wires in a bath containing dissolved cobalt sulphate and ammonium citrate at pH 9.8. The characteristics for the o.e.r. were determined in nonpurified 40 wt % KOH for temperatures ranging from 40° C to 80° C. The experimental conditions for preparing the cobalt electrodeposits were very similar to those used to obtain nickel black electrodes [6] except that the bath for the electrode preparation contained cobalt sulphate rather than the nickel sulphate used in [6]. Nickel was used as a substrate because of its excellent chemical stability in concentrated alkaline solutions. It is also a parent metal of cobalt and cheaper. Furthermore, since the substrate is different in nature from the electrodeposited metal, the amount of deposited cobalt on nickel can easily be determined.

2. Experimental details

Vertical nickel wires (99.99%) 0.05 cm in diameter were masked with Teflon tape, except for a 1 cm length at the bottom, to present an electrode surface of 0.157 cm^2. The samples were not exposed to heat treatment (and were not sealed directly into glass) prior to the cobalt deposition. They were successively polished with ~0.3 μm of alumina paste, rinsed with distilled water, briefly etched in a 1 : 4 HNO_3 solution and again rinsed with distilled water. In a first set of experiments, the samples were immersed in a bath of cobalt sulphate ($CoSO_4 \cdot 7H_2O$) 11.2 g dm^{-3} and ammonium citrate 92.4 g dm^{-3}, while ammonium hydroxide was added to obtain a pH of 9.8. The temperature of the bath was 23° C and a constant cathodic current density of 0.02 A cm^{-2} was applied during a given time, t_p, ranging from 0 to 3 h to form the deposit. The solution was not mechanically agitated during the formation of the coating. To determine the amount of deposited cobalt, the samples were rinsed and dissolved in 1 : 4 HNO_3, and the cobalt content of this solution was determined by optical emission spectroscopy with induced coupled plasma. The cobalt deposition rate was calculated from the amount of deposited cobalt against t_p. The effect of the cathodic current density, the concentration of dissolved cobalt and the temperature of the bath on the cobalt deposition rate also were investigated.

The cell used for the electrochemical measurements is described in detail elsewhere [7, 8]. The temperature ranged from 40 to 80° C; it was maintained constant by means of a Lauda M 20 thermostatic bath. The non-purified and deareated 40 wt % KOH solutions contained ~1 p.p.m. dissolved iron. After removal of the sample from the electrodeposition bath, it was rinsed with distilled water and immersed in the very concentrated alkaline solution. The electrochemical measurements for the o.e.r were carried out by applying a constant anodic current density of 1 A cm^{-2} for 0.5 h before reducing the current galvanostatically from 1 to 10^{-4} A cm^{-2}. Tafel lines were obtained after

0021-891X

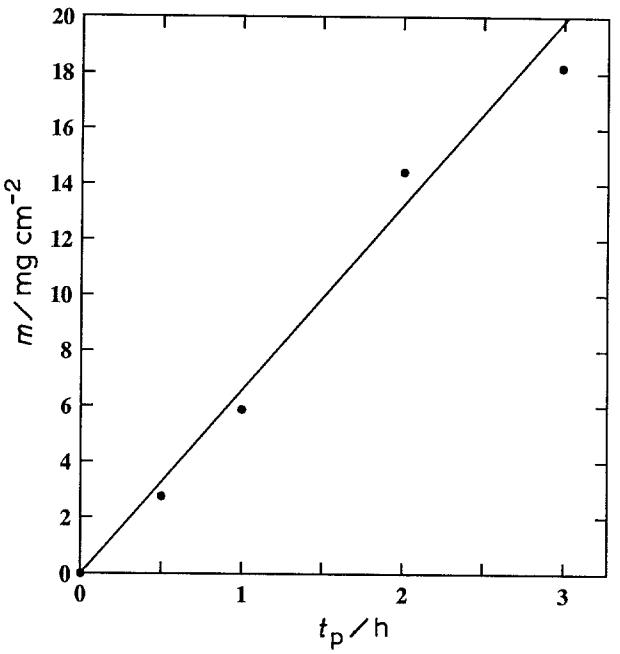

Fig. 1. Amount of deposited cobalt (m) against t_p (T = 23° C, i_a = 0.02 A cm^{-2}, [Co] = 0.04 M).

correction of the oxygen overpotentials (η_{O_2}) for the ohmic drop by the current-interruption technique.

The potentials were measured against a Hg|HgO|40 wt % KOH reference electrode at the bath temperature. The experimental value of the reversible potential for the hydrogen evolution reaction in 40 wt % KOH was then obtained at the different working temperatures with respect to this electrode. Finally, the reversible potentials for the o.e.r. with respect to the same reference electrode were calculated at each temperature by adding the reversible voltage for the decomposition of water to the measured values of the reversible potential for the hydrogen evolution reaction.

3. Results

3.1 *Coating characteristics*

The amount of electrodeposited cobalt on nickel substrate, m, is given against t_p in Fig. 1 (T = 23° C, i_a = 0.02 A cm^{-2}, [Co] = 0.04 M). A linear relationship of m against t_p is observed with a slope of 1.69 μg cm^{-2} s^{-1}. A faradic efficiency of ~28% is deduced for an applied cathodic current density of 0.02 A cm^{-2} from the slope value of m against t_p in Fig. 1; it is assumed that cobalt (II) species are present in the solution. This low faradic efficiency suggests that hydrogen evolution occurs during the electrode preparation.

It was noted that the cobalt deposition rate (i.e. the slope dm/dt_p) largely increases when the applied cathodic current (i_a) is raised from 0.002 to 0.1 A cm^{-2}. The following relationship between dm/dt_p and i_a was found (T = 23° C, [Co] = 0.04 M):

Table 1. Faradic efficiency for cobalt deposition for different concentrations of dissolved cobalt (T = 23° C, i_a = 0.04 A cm^{-2})

[Co]/M	*Faradic efficiency*/%
0.0036	3.5
0.007	7.2
0.014	12
0.04	28
0.07	30
0.142	44

$$\frac{dm}{dt_p} = 2.4 \times 10^{-5} \times i_a^{0.7} (0.05 \leqslant i_a \leqslant 0.1\,\text{A cm}^{-1}) \quad (1)$$

where dm/dt_p is in g s^{-1} cm^{-2} and i_a in A cm^{-2}. The faradic efficiency is equal to about 28% at 0.005 A cm^{-2} and decreases slightly with i_a for i_a > 0.005 A cm^{-2}; e.g. at i_a = 0.1 A cm^{-2} it is about 16%. Both the cobalt deposition rate and the faradic efficiency are also linked to the concentration of dissolved cobalt. For the former, the following relationship (T = 23° C, i_a = 0.02 A cm^{-2}) is found:

$$\frac{dm}{dt_p} = 1.03 \times 10^{-5} \times [\text{Co}] \quad (3.6 \times 10^{-3}\,\text{M} \leqslant [\text{Co}] \leqslant 0.14\,\text{M}) \quad (2)$$

where dm/dt_p is in g s^{-1} cm^{-2} and [Co] in mole dm^{-3}. An increase of [Co] results in a large improvement of the faradic efficiency (Table 1). It was further established that the deposition rate at i_a = 0.02 A cm^{-2} and [Co] = 0.04 M is only slightly dependent on the temperature, since dm/dt_p = 1.74 μm cm^{-2} s^{-1} at 35°C compared to 1.90 μm cm^{-2} s^{-1} at 75° C.

The coating morphology was investigated by scanning electron microscopy (SEM) for a deposition time of up to 3 h (T = 23° C, i_a = 0.2 A cm^{-2}, [Co] = 0.04 M). The deposit takes the form of nodules with a diameter of ~6 μm for the larger ones when m = 2.6 mg cm^{-2} (Fig. 2a). The size of the cobalt nodules increases with m to reach a diameter of 15–20 μm for the larger ones when m = 18 mg cm^{-2} (Fig. 2b–d).

For a cobalt loading of 2.5 mg cm^{-2}, it was observed that the morphology of the coating depends slightly on both the applied cathodic current density (0.002 ⩽ i_a ⩽ 0.1 A cm^{-2}) and the concentration of dissolved cobalt (0.0036 ⩽ [Co] ⩽ 0.14 M). However, the lower i_a, the better the mechanical stability of the deposit. In addition, the morphology of the coating is quite different at 23° C and 75° C with i_a = 0.02 A cm^{-2} and [Co] = 0.04 M.

The surface roughness values were estimated on a relative scale for cobalt loading up to 18 mg cm^{-2}. The electrodeposition was carried out at T = 23° C under a current density of 0.02 A cm^{-2} in the presence of 0.04 M dissolved cobalt. After electrode preparation, the samples were rinsed in distilled water and immersed in 40 wt % KOH at 80° C. A potential of −0.08 V vs RHE was applied for several minutes before potential scanning in the anodic direction (from −0.08 V vs

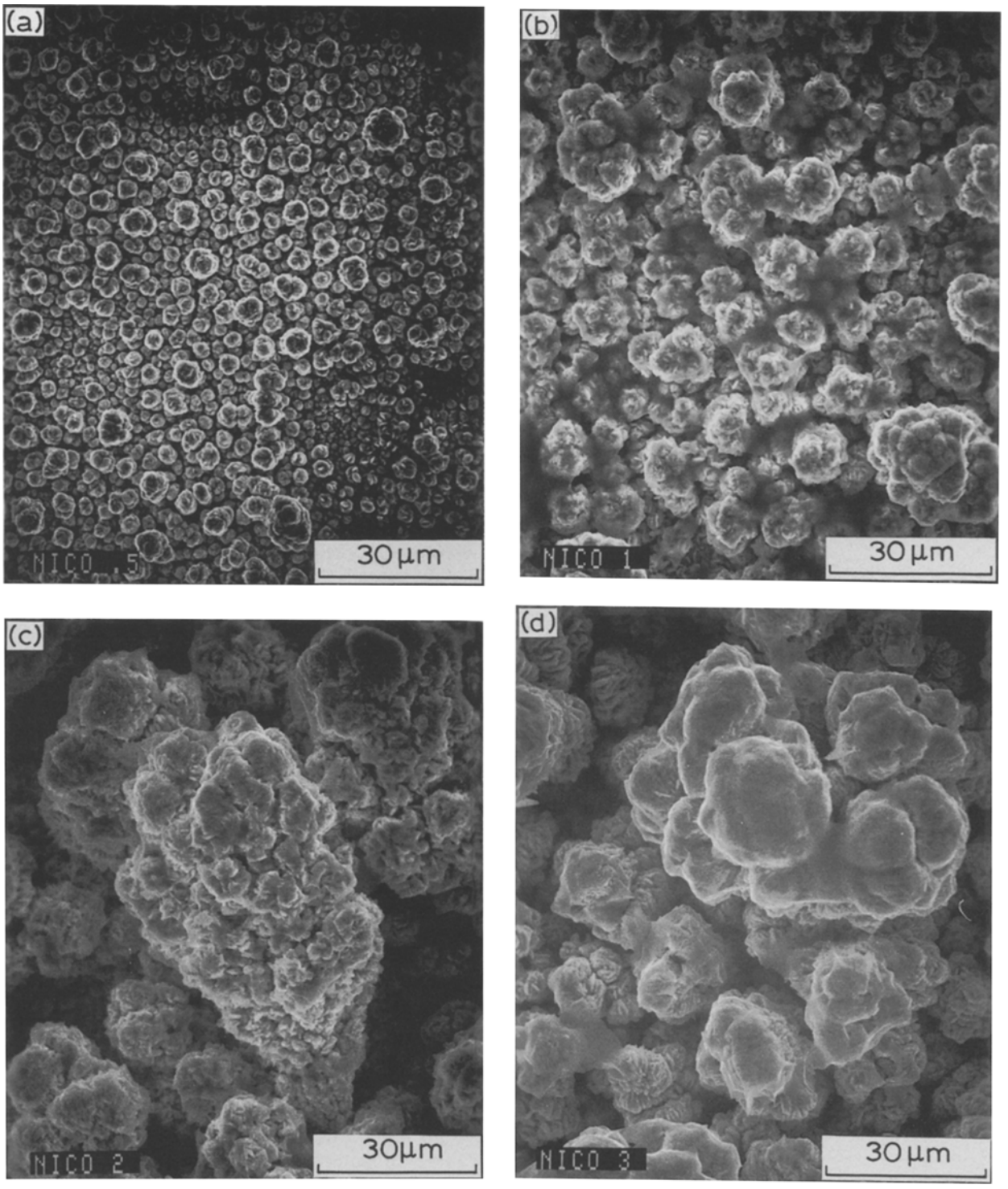

Fig. 2. SEM pictures after cobalt deposition for m: (a) 2.6, (b) 6.0, (c) 12, and (d) 18 mg cm^{-2}. The samples were prepared according to Fig. 1.

RHE to +0.92 V vs RHE) at a sweep rate of 0.001 Vs^{-1}. For a pure cobalt wire electrode (m = 0) and a cobalt loading up to 18 mg cm^{-2}, the potentiodynamic curves displayed an anodic peak at +0.17–+0.22 V vs RHE, which corresponds to the oxidation of Co to Co(II) species (i.e. CoO/Co(OH)$_2$) ([9] and reference therein).

If it is assumed that under this oxidation peak the charge (Q_{POX}) is linked to the roughness factor of the electrode surface, the surface roughness values may be estimated on a relative scale from the ratio $(Q_{POX})_m/(Q_{POX})_{m=0}$. It should be noted that $(Q_{POX})_m$ is Q_{POX} for a given loading; $(Q_{POX})_{m=0}$ is Q_{POX} at m = 0 for a pure cobalt wire electrode. The ratio $(Q_{POX})_m/(Q_{POX})_{m=0}$ is plotted against m in Fig. 3. A small increase in the ratio is observed from m = 0 to 2.6 mg cm^{-2} but the enlargement is significant from m = 2.6 to 12 mg cm^{-2}. Thereafter, the variation is negligible up to 18 mg cm^{-2}.

3.2 *O.e.r. at 80° C*

The current density is plotted on a logarithmic scale against the oxygen overpotential in Fig. 4 for m = 0, 2.6 or 18 mg cm^{-2}. A break in the Tafel slope is noted

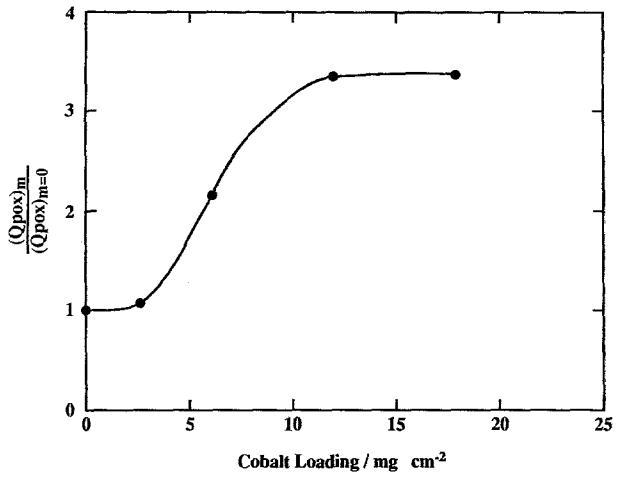

Fig. 3. Ratio $(Q_{POX})_m/(Q_{POX})_{m=0}$ against the cobalt loading. Sample preparation: according to Fig. 1. $(Q_{POX})_m$ values were obtained from the first oxidation peak on the voltammetric curves recorded at 0.001 V s^{-1}.

at $\eta_{O_2} \sim 0.26$ V for bare nickel anodes compared to $\eta_{O_2} \sim 0.22$ V for a cobalt loading of 2.6–18 mg cm^{-2}. In all cases, the Tafel slope increases from low to high η_{O_2} values. The Tafel parameters obtained under the experimental conditions in Fig. 4 are summarized in Table 2 for m values up to 18 mg cm^{-2}. The current density at $\eta_{O_2} = 0.3$ V ($i_{0.3}$) or $\eta_{O_2} = 0.2$ V ($i_{0.2}$) is also given for each loading. In the region of high η_{O_2}, the Tafel slope (b) decreases and the exchange current

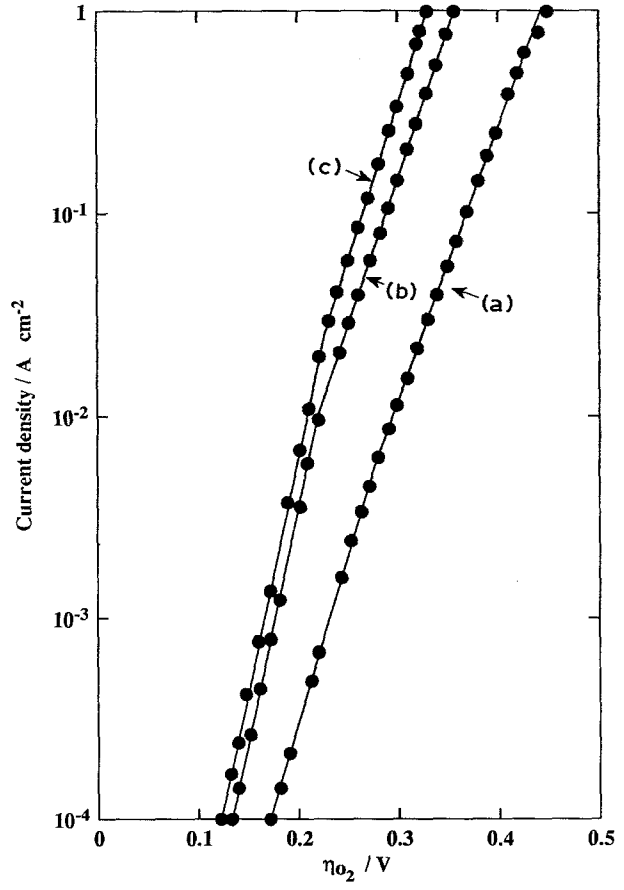

Fig. 4. Tafel lines for the o.e.r. (*IR*-corrected) after a preanodization time of 30 min under an anodic current density of 1 A cm^{-2} in 40 wt % KOH at 80° C. Pure nickel with m: (a) 0, (b) 2.6, and (c) 18 mg cm^{-2}. Sample preparation: according to Fig. 1.

density (i_0) increases from $m = 0$ to 2.6 mg cm^{-2}; the electrocatalytic activity at 0.3 V i.e. $i_{0.3}$ improves considerably. The variation of i_0, b and $i_{0.3}$ is small from $m = 2.6$ to 12 mg cm^{-2} and all three parameters are constant for m ranging from 12 to 18 mg cm^{-2}.

In the region of low η_{O_2}, the improved electrocatalytic activity from $m = 0$ to 2.6 mg cm^{-2} is due to the large decrease of b. Since b is practically constant in the range from $m = 2.6$ to 18 mg cm^{-2}, the small variation of $i_{0.2}$ with m is mainly linked to the small variation in i_0 with m.

The potentiodynamic traces recorded after the o.e.r. on cobalt coatings display two reduction peaks (labelled I and II in Fig. 5). A preanodization current of 1 A cm^{-2} was applied for 30 min before the potential sweep in the cathodic direction. It is noted that the height of peaks I and II is strongly related to the loading. Peak I is located at ~0.85 V vs RHE (*IR*-corrected) while peak II is at ~0.5 V vs RHE (*IR*-corrected); their location is practically independent of the loading from 2.6 to 18 mg cm^{-2}. The total charge (Q_{RED}) related to the reduction peaks and the shoulder at ~1.32 V vs RHE, from the potentiodynamic traces of Fig. 5, is plotted against m and $(Q_{POX})_m/(Q_{POX})_{m=0}$ in Fig. 6. It is observed that the rate of increase of Q_{RED} with $m(dQ_{RED}/dm)$ is ~317 C g^{-1} for $m < 6$ mg cm^{-2}, compared to ~50 C g^{-1} for $m >$ 12 mg cm^{-2}.

The current density at $\eta_{O_2} = 0.3$ V (Table 1) is plotted against Q_{RED} and $(Q_{POX})_m/(Q_{POX})_{m=0}$ in Fig. 7. Note that $i_{0.3}$ increases almost linearly with the latter ratio and the amount of reducible oxide(s)/hydroxide(s) species at a rate of 0.14 A C^{-1} up to $Q_{RED} = 2$ C cm^{-2} (Fig. 7a).

In further sets of experiments, the samples in the preparation bath were obtained under different experimental conditions (i_a, [Co], T) to obtain 2.5 mg cm^{-2} cobalt loadings with a different morphology. The kinetic parameters for the o.e.r. were not dependent on the coating morphology.

3.3. *Influence of the temperature during electrolysis*

The o.e.r. kinetic parameters and the current density for $\eta_{O_2} = 0.3$ V ($i_{0.3}$) or 0.15 V ($i_{0.15}$) are summarized in Table 3 for temperatures ranging from 40 to 80° C and a cobalt loading of 12 mg cm^{-2}. From 80 to 40° C, a slight decrease in b and a considerable decrease in both i_0 and $i_{0.3}$ are noted in the region of high η_{O_2}. The apparent energy of activation ($\Delta H^{\neq}$) was calculated from Arrhenius plots of log $i_{0.3}$ against T^{-1}. Below 60° C, $\Delta H^{\neq}$ is equal to 30 kJ mol^{-1} compared to 105 kJ mol^{-1} above 60° C.

In the region of low η_{O_2}, the lower the temperature, the larger the Tafel slope and the lower the $i_{0.15}$. The variation of i_0 with the temperature is very small in the latter region compared to the region at high η_{O_2}. $\Delta H^{\neq}$, calculated from the log $i_{0.15}$ against T^{-1} plot, is equal to 50 kJ mol^{-1} (40–80° C).

Potentiodynamic traces were recorded after 30 min under a preanodization current of 1 A cm^{-2}, the

*Table 2. Kinetic parameters of the o.e.r. at 80° C for different cobalt loadings**

	Low η_{O_2}			*High* η_{O_2}		
m/mg cm^{-2}	i_0/A cm^{-2}	b/V dec^{-1}	$i_{0.2}$/A cm^{-2}	i_0/A cm^{-2}	b/V dec^{-1}	$i_{0.3}$/A cm^{-2}
2.6	1.1×10^{-7}	0.044	3.7×10^{-3}	5.8×10^{-6}	0.068	0.15
6.0	2.1×10^{-7}	0.044	7.3×10^{-3}	6.4×10^{-6}	0.065	0.25
12	1.3×10^{-7}	0.042	7.6×10^{-3}	10×10^{-6}	0.066	0.35
18	1.4×10^{-7}	0.043	6.6×10^{-3}	8.9×10^{-6}	0.065	0.35
Ni wire ($m = 0$)	1.0×10^{-7}	0.057	0.33×10^{-3}	1.0×10^{-6}	0.074	0.01

* Sample preparation: $T = 23°$ C, $i_a = 0.02$ A cm^{-2}, [Co] = 0.04 M

cobalt loading being 12 mg cm^{-2}. The temperature was maintained constant at 40, 50, 60, 70 or 80° C. The potentiodynamic traces obtained at 40 and 70° C are illustrated in Fig. 8. The shape of the curves is practically unchanged from 40 to 80° C (curve c, Fig. 5). However, the height of peak II decreases considerably from 80 to 40° C while peak I predominates at 70° C and below. The location of peak I is practically independent of the temperature. In addition, the total charge of reduction tends to decrease as T is lowered but Q_{RED} is not really reproducible at 60° C and below.

4. Discussion

4.1. *O.e.r. at 80° C*

For a smooth polished cobalt electrode in 4.8 M KOH solution at 25° C [10] a Tafel slope of $0.66 \times 2.3RTF^{-1}$ was found in the region of low η_{O_2} (~ 0.24 V $< \eta_{O_2} <$ ~ 0.3 V) compared to $2.3RTF^{-1}$ in the region of high η_{O_2} ($\eta_{O_2} > 0.3$ V) with regard to the o.e.r. The former slope is compatible with two mechanisms [10–12], the first rate-determining step (r.d.s.) is:

$$CoO_2 + O_{ad}^- \longrightarrow CoO_2 \cdot O + e^- \quad (3)$$

The r.d.s. of the second step is:

$$CoOOH + OH^- \longrightarrow CoO_2 + H_2O + e^- \quad (4)$$

A slope value of $\sim 2.3RTF^{-1}$ is found for a mechanism having the following r.d.s. [12]:

$$M - OH + OH^- \longrightarrow M - O^- + H_2O \quad (5)$$

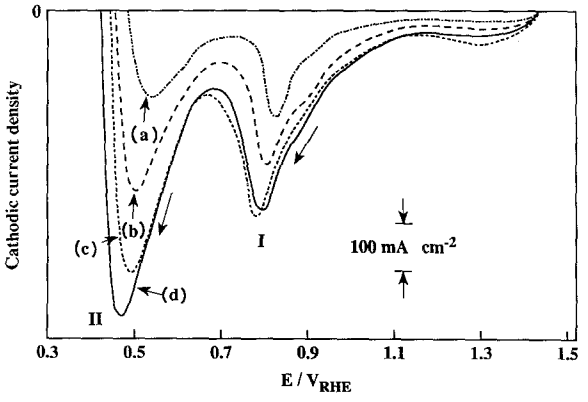

Fig. 5. Poteniodynamic traces after 30 min preanodization under 1 A cm^{-2} for different cobalt loadings (40 wt % KOH, 80° C sweep rate: 0.1 V s^{-1}; potentials not *IR*-corrected). m: (a) 2.6, (b) 6.0, (c) 12, and (d) 18 mg cm^{-2}. Sample preparation according to Fig. 1.

In the region of high η_{O_2} at 80° C, it is deduced that the r.d.s. on a cobalt coating corresponds to Reaction 5 since b is $\sim 0.95 \times 2.3RTF^{-1}$ (Table 2). A Tafel slope of $\sim 0.62 \times 2.3RTF^{-1}$ in the region of low η_{O_2} at 80° C suggests that Reaction 3 or 4 is the rate-determining step.

The potentiodynamic curves (Fig. 5) recorded after preanodization of the cobalt coating are consistent with the potentiodynamic behaviour reported for nonporous [11, 13] or porous [4, 14] cobalt in alkaline solution. The shoulder located at ~ 1.32 V vs RHE is ascribed to the reduction of CoOOH to $Co(OH)_2$, peak I to the reduction of Co_3O_4 (i.e. a mixture of Co(+2) and Co(+3) species) to $Co(OH)_2$ and peak II to the reduction of $Co(OH)_2$ to cobalt [4, 9, 14]. Since the charge linked to peak I is large compared to the one associated with the shoulder, it is deduced that the amount of Co_3O_4 exceeds the amount of CoOOH.

As postulated by Conway and Liu [15], Co(III) and Co(IV) states can be involved at the Co_3O_4 external surface and the variation of the surface density ratio Co(III)/Co(IV) may explain the change of the r.d.s. for the o.e.r. from high to low η_{O_2} values through a Conway–Bourgault mechanism [16].

An alternative explanation for the break in the Tafel slope at $\eta_{O_2} \sim 0.22$ V (cf., Fig. 4) and hence the

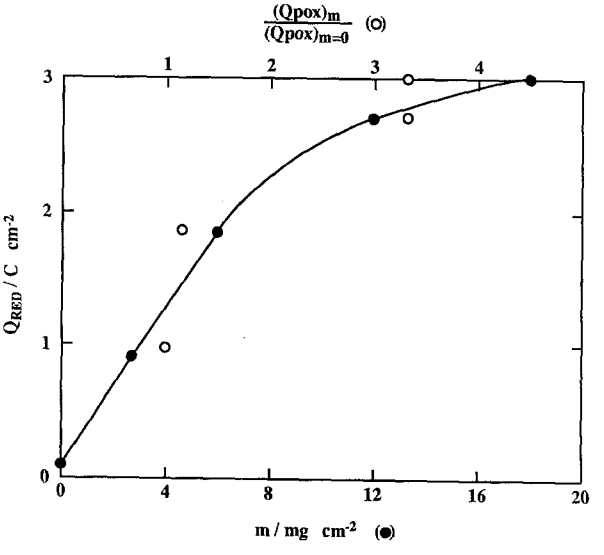

Fig. 6. The charge (Q_{RED}), corresponding to the reduction peaks plus the shoulder, against m and $(Q_{POX})_m^*/(Q_{POX})_{m=0}^*$. The other experimental conditions are those of Fig. 5 (*: from Fig. 3).

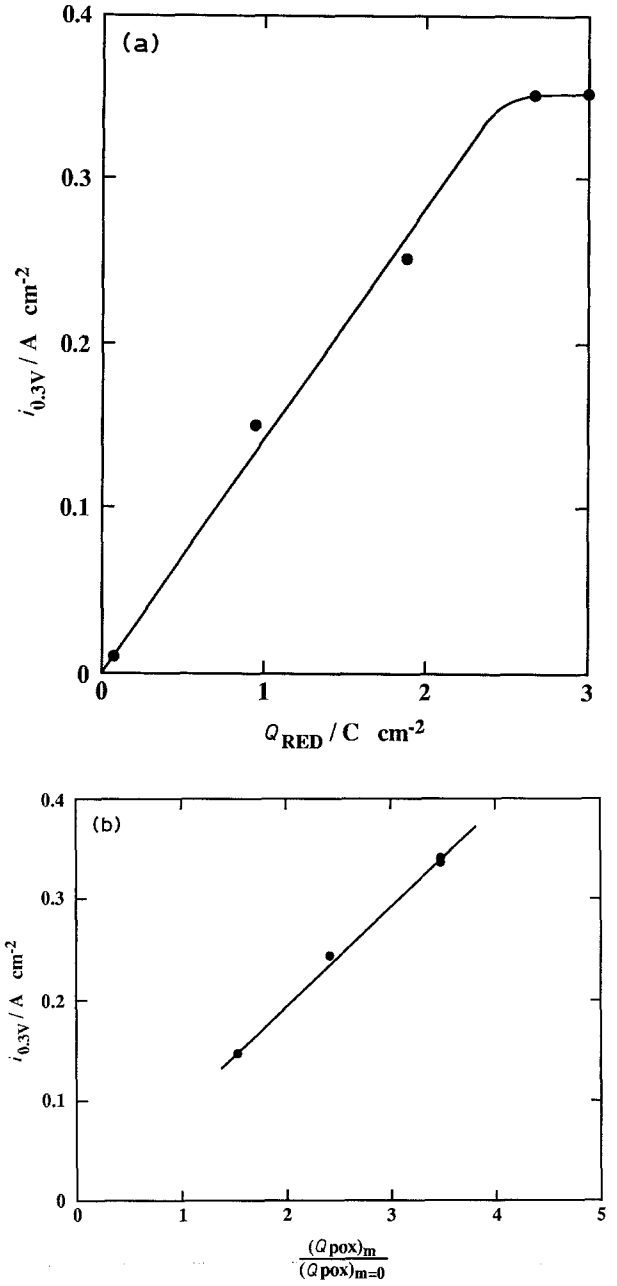

Fig. 7. $i_{0.3}$ against Q_{RED} and the ratio of $(Q_{POX})_m/(Q_{POX})_{m=0}$. $i_{0.3}$ values are those summarized in Table 1. Q_{RED} values were determined from the potentiodynamic traces in Fig. 5. Ratios $(Q_{POX})_m/(Q_{POX})_{m=0}$ are given in Fig. 3.

change in reaction mechanism, is deduced from the views of Tseung and Jasem ([17] and references therein) who pointed out the role of higher/lower oxidation state couples for metal-oxide electrodes in the oxygen evolution reaction. It may be that only those cobalt cations in the highest oxidation state (corresponding to the charge under the shoulder at 1.32 V vs RHE) give rise to fast oxygen evolution rates. The remaining 'surface' cations in lower oxidation states may be more sluggish for the o.e.r. until high overpotentials are reached and a break in the Tafel slope may result.

As far as variation of the electrocatalytic activity with loading is concerned, the increase of current density at $\eta_{O_2} = 0.3$ V with m (Table 2) is related to the fact that the electrode/solution interface increases from $m = 2.6$ to 12 mg cm^{-2}, as manifested by a significant enlargement of the ratio $(Q_{POX})_m/(Q_{POX})_{m=0}$ with m in this loading range (Fig. 3). Since the r.d.s. of the o.e.r. is a surface reaction, the linear variation of $i_{0.3\,V}$ with the ratio $(Q_{POX})_m/(Q_{POX})_{m=1}$ (Fig. 7b) is not surprising. Furthermore, the larger the electrode/solution interface, the greater the charge of reduction (Fig. 6).

4.2. *Influence of the temperature during electrolysis*

It is deduced that the r.d.s. of the o.e.r. is not dependent on temperature in the region of high η_{O_2} since b remains at $\sim 2.3RTF^{-1}$ between 40 and 80° C (Table 3). The fact that the apparent energy of activation is 30 kJ mol^{-1} below 60° C compared with 105 kJ mol^{-1} above 60° C (high η_{O_2}) is probably related to changes in the amount of reducible oxide(s)/hydroxide(s) species with temperature (Figs 5c, 8).

In the region of low η_{O_2}, b decreases from $2.3RTF^{-1}$ at 40° C to $\sim 0.6 \times 2.3RTF^{-1}$ at 80° C (Table 3), which probably means that there is a slight difference in the o.e.r. mechanism in relation to the temperature, although the exact nature of this difference is not clearly understood.

The morphology of cobalt electrodeposits formed at 25° C on nickel substrate in 30 wt % KOH solutions containing tris-ethylenediamine cobalt chloride is quite different [3] from that of the cobalt deposits obtained in the present investigation (Fig. 2). The deposits contain a large number of holes (per unit area) surrounded by cobalt particles in the first case, while such holes are absent in the second. In addition, the mechanical stability of cobalt deposits is weaker in the first case.

With regard to the electrocatalytic activity for the o.e.r., $i_{0.3} = 0.13$ A cm^{-2} in 30 wt % KOH at 70° C for

*Table 3. Kinetic parameters of the o.e.r. at different temperatures for a cobalt loading of 12 mg cm^{-2}**

	Low η_{O_2}			*High* η_{O_2}		
T/° C	i_0/A cm^{-2}	b/V dec^{-1}	$i_{0.15}$/A cm^{-2}	i_0/A cm^{-2}	b/V dec^{-1}	$i_{0.3}$/A cm^{-2}
40	0.75×10^{-7}	0.054	0.45×10^{-4}	0.29×10^{-6}	0.062	0.022
50	2.0×10^{-7}	0.054	1.2×10^{-4}	1.1×10^{-6}	0.066	0.036
60	2.0×10^{-7}	0.053	1.4×10^{-4}	0.90×10^{-6}	0.064	0.044
70	2.0×10^{-7}	0.047	3.1×10^{-4}	7.2×10^{-6}	0.072	0.11
80	1.3×10^{-7}	0.042	4.9×10^{-4}	10×10^{-6}	0.066	0.35

* Sample preparations: $T = 23$° C, $i_a = 0.02$ A cm^{-2}, [Co] = 0.04 M

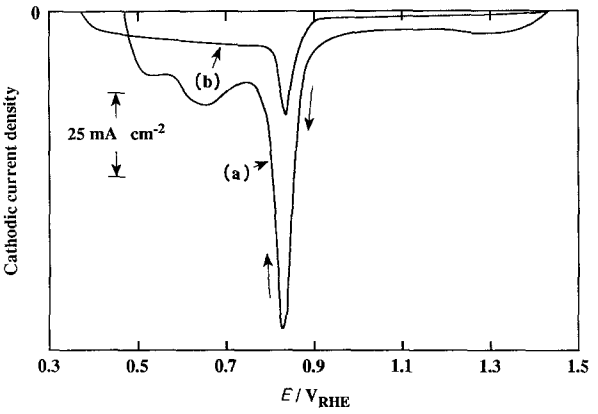

Fig. 8. Influence of the temperature on the potentiodynamic traces for a cobalt loading of 12 mg cm^{-2} at: (a) 70° C and (b) 40° C. Except for the temperature and loading, the experimental conditions are those of Fig. 5.

a cobalt loading of 4.6 mg cm^{-2} when prepared from tris-ethylenediamine cobalt chloride compared to 0.35 A cm^{-2} in 40 wt % KOH at 80° C (or 0.11 A cm^{-2} at 70° C) for a cobalt loading of 12 mg cm^{-2} when prepared from a solution at a pH of 9.8 (Table 3). The performances of different electrode materials recently developed for the o.e.r. in a highly concentrated alkaline solution at 70–80° C [3, 18–21] are summarized in Table 4. Any comparison of these performances should recognize that the experimental conditions may have been slightly different for each material during the o.e.r., e.g. the iron content of the solution, the electrolyte concentration and temperature, plus the preanodization current and time. Among the materials considered, anodes with electrodeposited cobalt on a nickel substrate (Tables 3 and 4) have good performances for the o.e.r. but Raney nickel/Co_3O_4 composite anodes are definitely superior [21].

The overpotential for the o.e.r. was recorded during six consecutive days for an electrode with a cobalt loading of 12 mg cm^{-2} in a 40 wt % KOH solution at 80° C. Under an applied current density of 1 A cm^{-2}, a 5 mV increase was noticed from 0.5 to 12 h but no further variation of the overpotential was observed after 12 h.

5. Conclusion

Cobalt coatings obtained on a nickel substrate under the experimental conditions of the present investigation (i.e. typically T = 23° C, i_a = 0.02 A cm^{-2}, [Co] = 0.04 M) take the form of nodules. The current efficiency is dependent on both the cathodic applied current density and the concentration of dissolved cobalt in the preparation bath. In 40 wt % KOH at 80° C, a dual Tafel region is observed on log current density versus overpotential curves; it is deduced that the rate-determining step of the o.e.r. is different in both regions. The current density at an overpotential of 0.3 V increases linearly with the amount of reducible oxide(s)/hydroxide(s) (up to ~2 C cm^{-2}) formed during preanodization at 80° C. Electrocatalytic activity decreases as the temperature is lowered.

Acknowledgements

The technical assistance of Dr E. Potvin and G. Larochelle of IREQ is gratefully acknowledged. One of the authors, C. Messier, was a student at Sherbrooke University (Québec, Canada) when this paper was written. The authors also thank Energy Mines and Resources Canada, who provided financial support through the Hydrogen Industry Council.

References

[1] C. T. Bowen, H. J. Davis, B. F. Henshaw, R. Lachance, R. L. Le Roy and R. Renaud, *Int. J. Hydrogen Energy* **9** (1984) 59.
[2] D. E. Hall, *J. Electrochem. Soc.* **132** (1985) 41.
[3] L. Brossard, *Mater. Chem. & Phys.* **27** (1991) 235.
[4] L. Brossard, *Int. J. Hydrogen Energy* **16** (1991) 87.
[5] A. Brenner, 'Electrodeposition of Alloys', Academic Press, New York (1963) Vol. II, Chap. 31.
[6] A. C. Chialvio, M. R. Gennero de Chialvio, *J. Appl. Electrochem.* **21** (1991) 440.
[7] J. Y. Huot and L. Brossard, *Surf. & Coat. Technol.* **34** (1988) 373.
[8] J. Y. Huot and L. Brossard, *Int. J. Hydrogen Energy* **12** (1987) 821.
[9] T. R. Jayaraman, V. K. Venkatesan and H. V. K. Udupa, *Electrochim. Acta* **20** (1975) 209.
[10] H. Willems, A. G. C. Kobussen, J. H. W. De Wit and G. H. J. Broers, *J. Electroanal. Chem.* **17** (1984) 227.
[11] L. D. Burke, M. E. Lyons and O. J. Murphy, *J. Electronal. Chem.* **132** (1982) 247.

Table 4. Performances of different electrode materials for the o.e.r. in highly concentrated alkaline solution at 70–80° C.

Material	b/V dec^{-1}	i_0/A cm^{-2}	$i_{0.3}$/A cm^{-2}	*Reference*
Raney Ni*	0.080	5.2 × 10^{-6}	0.029	[18]
Raney Ni–Co*	0.055	4.7 × 10^{-8}	0.013	[18]
Raney Co*	0.054	3.3 × 10^{-8}	0.012	[18]
Electrodeposited Co*† on a nickel substrate loading: 4.6 mg cm^{-2}	0.054	3.7 × 10^{-7}	0.130	[3]
CoOOH/Co_3O_4‡ on a nickel substrate	0.062	3.1 × 10^{-6}	0.210	[19]
Ni–Fe*	0.088	3.7 × 10^{-5}	0.095	[20]
Raney Ni/Co_3O_4 composite anodes	not available	not available	larger than 1 A cm^{-2}	[21]

* The o.e.r. kinetic parameters reported here correspond to the best performance of the material under consideration in the region of high potentials.
† Cobalt was electrodeposited in the presence of tris-ethylenediamine cobalt (III) chloride in 30 wt % KOH aqueous solutions.

[12] R. Rasiyak, A. C. C. Tseung and D. B. Hibbert, *J. Electrochem. Soc.* **129** (1982) 1724.
[13] F. Hahn, B. Beden, M. J. Croissant and C. Lamy, *Electrochim. Acta* **31** (1986) 335.
[14] L. Brossard, *Mater. Chem. & Phys.* **30** (1992) 267.
[15] B. F. Conway and T. C. Liu, *ibid.* **22** (1989) 163.
[16] B. E. Conway and P. L. Bourgeault, *Can. J. Chem* **37** (1959) 292.
[17] A. C. C. Tseung and S. M. Jasem, *Electrochim. Acta* **22** (1977) 31.
[18] Y. Choquette, H. Ménard and L. Brossard, *Int. J. Hydrogen Energy* **15** (1990) 21.
[19] L. Brossard, *J. Appl. Electrochem.* **21** (1991) 612.
[20] E. Potvin and L. Brossard, *Mater. Chem. & Phys.* **31** (1992) 311.
[21] G. Schiller and V. Borck, *Int. J. Hydrogen Energy* **17** (1992) 261.